The CHIANTI Atomic Database: New Improvements for Solar Physics Applications

Peter R. Young[1*], Giulio Del Zanna[2], Ken P. Dere[1], Enrico Landi[3], Helen E. Mason[2]

([1]George Mason University, Fairfax, VA; [2]Cambridge University, Cambridge, UK; [3]University of Michigan, Ann Arbor, MI)

(*Work funded by NASA through a contract with the US Naval Research Laboratory)

1. The CHIANTI atomic database

CHIANTI is an atomic data and software package for modeling emission lines and continuum from optically thin plasmas. The first version was released in 1996 (Dere et al. 1997) and the most recent version (7) was released in 2011 (Landi et al. 2012). A further update will be released in 2012, which we refer to as CHIANTI 7.1. **Table 1** shows the major ions that will be in CHIANTI 7.1.

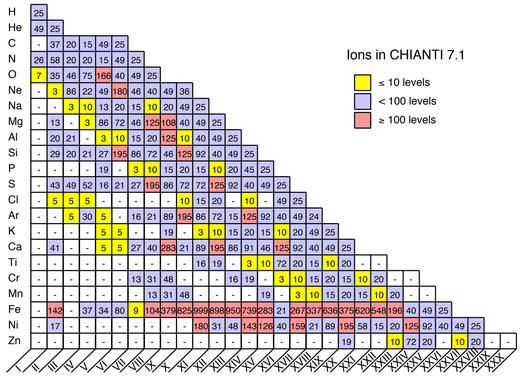

Table 1: Table showing the ions of the major elements that will be present in CHIANTI 7.1. The numbers for each entry give the numbers of atomic levels for each ion.

2. The coronal iron ions

The coronal iron ions are considered here to be Fe IX through XVII, which are formed at temperatures between 1 and 5 MK in electron ionized plasmas, and are a prominent feature of spectra from the solar corona. Atomic data improvements over the past decade have focused on:

1. Accurate R-matrix calculations for the lowest-lying levels that give rise to the strongest transitions.
2. Large distorted wave (DW) calculations for 100's of levels belonging to higher energy configurations.

The former are very important for the Hinode/EIS mission, which obtains high resolution spectra of many of the strongest transitions from coronal iron ions. They are also important for SDO/AIA which has image filters centered on key iron transitions such Fe IX λ171.07, Fe XII λ195.12 and Fe XVI λ360.76.

The DW calculations are important for filling out the solar spectrum with large numbers of weak transitions, particularly in the soft X-ray wavelength region. These lines contribute to the bandpasses of SDO/AIA, and also to the wide spectral range covered by the SDO/EVE irradiance experiment.

One surprise from comparisons of the new atomic data with X-ray spectra (Del Zanna 2012) is that R-matrix calculations are required for n=4 levels in the coronal iron ions, and CHIANTI 8 will contain this new set of data.

The status of the electron excitation data-sets for the coronal iron ions, as scheduled for CHIANTI 7.1, is summarized in **Table 2**.

Ion	CHIANTI update version	Data-sets	Type
Fe IX	5	Storey et al. (2002)	R-matrix
	7.1	O'Dwyer et al. (2012)	DW
Fe X	5	Del Zanna et al. (2004)	R-matrix
	7.1	Landi & Dere (2012)	DW
Fe XI	7.0	Del Zanna et al. (2010)	R-matrix
	7.1	Landi & Dere (2012)	DW
Fe XII	5	Storey et al. (2005)	R-matrix
	7.1	Landi & Dere (2012)	DW
Fe XIII	7.0	Storey & Zeippen (2010)	R-matrix
	7.1	Landi & Dere (2012)	DW
Fe XIV	7.0	Liang et al. (2010)	R-matrix
	7.1	Landi & Dere (2012)	DW
Fe XV	5.0	Berrington et al. (2005)	R-matrix
	7.1	Landi (2011)	DW
Fe XVI	1.0	Sampson et al. (1990)	DW
Fe XVII	7.0	Liang & Badnell (2010)	R-matrix
	5.0	Landi & Gu (2006)	DW

Table 2: A summary of the electron excitation data-sets that will be included in CHIANTI 7.1 for the coronal iron ions.

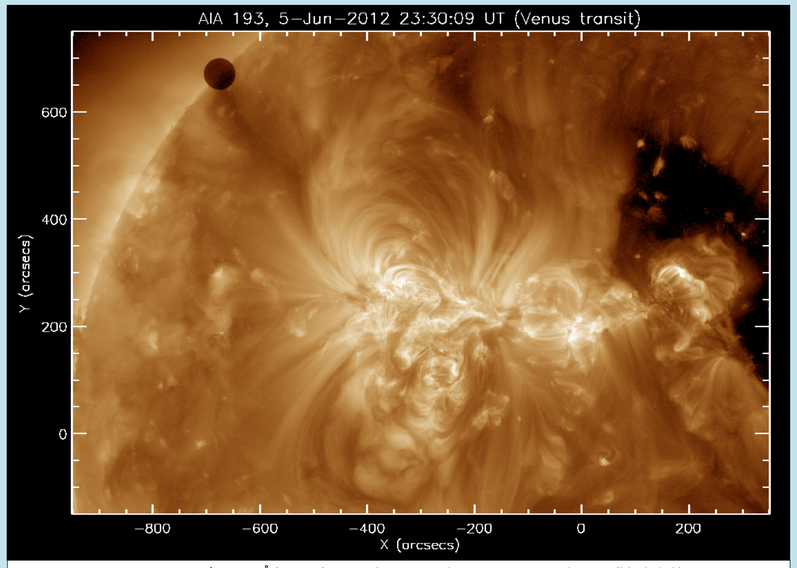

Figure 3: A SDO/AIA 193 Å (1.5 MK) image showing a solar active region and Venus (black disk).

3. Atomic data for Hinode/EIS

The EUV Imaging Spectrometer (EIS) was launched on board the *Hinode* satellite in 2006 and it returns spectra in the wavelength ranges 170-212 and 245-292 Å. The spectra are a huge advance on previous observations in these wavelength ranges and have revealed previously unidentified lines and discrepancies in atomic data that have been a challenge to spectroscopists.

3.1 Unidentified lines

The previously unidentified lines in EIS spectra (**Table 2**) are quite strong and form useful diagnostics.

Table 3: Strong lines identified from EIS spectra.

Ion	Wavelength	Transition	Reference
Fe IX	188.50, 189.94, 191.22	$3s^23p^53d\ ^3F_{2,3,4} - 3s^23p^4(^3P)3d^2\ ^3G_{3,4,5}$	Young (2009)
Fe IX	197.86	$3s^23p^53d\ ^1P_1 - 3s^23p^54p\ ^1S_0$	Young (2009)
Fe XI	202.42	$3s^23p^4\ ^3P_2 - 3s^23p^3(^2P)3d\ ^3P_2$	Del Zanna (2010)
Fe XI	256.92	$3s^23p^4\ ^3P_2 - 3s^23p^3(^4S)3d\ ^5D_4$	Del Zanna (2010)

3.2 Density diagnostics

The high effective area of EIS means that diagnostics such as Fe XII λ186.88/λ195.12 and Fe XIII λ203.82/λ202.04 allow the density to be derived with unprecedented precision, making the creation of density maps a routine procedure (**Figure 1**). However, this high precision has revealed discrepancies between different ions and diagnostics. The most striking difference is that between the Fe XII and Fe XIII diagnostics, and **Figure 2** shows how the densities derived from a quiet Sun data-set have changed with each new version of CHIANTI.

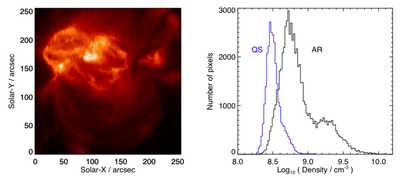

Figure 1: The left panel shows an active region density map derived from the Fe XIII λ203.82/λ202.04 ratio, and the right panel shows a histogram of density values (black line) derived from this map. The blue line shows a histogram derived from quiet Sun data.

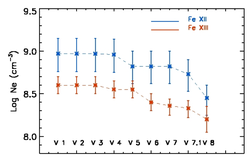

Figure 2: This plot shows how the density derived from a single, quiet Sun off-limb data-set has changed with time using the Fe XII λ186.88/λ195.12 and Fe XIII λ203.82/λ202.04 density diagnostics. the changes are due to atomic data models in CHIANTI.

References

Aschwanden & Boerner 2011, ApJ, 732, 81
Berrington et al. 2005, J. Phys. B, 38, 1667
Del Zanna 2010, A&A, 514, A41
Del Zanna 2012, arXiv:1208.2142v1
Del Zanna et al. 2004, A&A, 422, 731
Del Zanna et al. 2010, A&A, 514, A40
Dere et al. 1997, A&AS, 125, 149
Landi 2011, ADNDT, 97, 587
Landi & Dere, 2012, ADNDT, submitted
Landi & Gu, 2006, ApJ, 640, 1171
Landi et al., 2012, ApJ, 744, 99
Liang & Badnell 2010, A&A, 518, A64
Liang et al., 2010, ApJS, 190, 322
O'Dwyer et al. 2012, A&A, 537, 22
Sampson et al. 1990, ADNDT, 44, 209
Storey & Zeippen, 2010, A&A, 511, A78
Storey et al. 2002, A&A, 394, 753
Storey et al. 2005, A&A, 433, 717
Testa et al. 2012, ApJ, 745, 111
Young 2009, ApJ, 707, 173

4. SDO/AIA observations – the 94 Å filter

The AIA instrument obtains spectacular images (**Figure 3**) of the Sun in seven EUV filters centered at 94, 131, 171, 193, 211, 304 and 335 Å. Accurate atomic data are crucial not only for deriving physical parameters from the data, but even for simply interpreting the morphology of the images.

A particular challenge has the been the 94 Å filter which was chosen as it contains the strong Fe XVIII 93.93 Å emission line, which becomes prominent in flare spectra. However, quiet Sun and active region images clearly demonstrate that the filter contains cooler emission, and early work suggested that CHIANTI 6 underestimates this emission by a factor 7 (Aschwanden et al. 2011).

New atomic calculations performed for CHIANTI (Del Zanna 2012) demonstrate contributions from Fe VIII, X and XIV lines, the latter in particular being significant for active regions (**Figure 4**, **Table 4**).

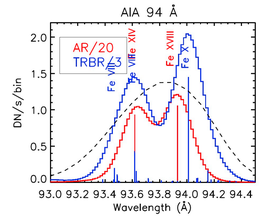

Table 4: Lines that contribute to AIA 94 Å channel.

Ion	Wavelength	Temperature
Fe VIII	93.469, 93.616	$3p^63d\ ^2D_{3/2,5/2} - 3p^67f\ ^2F_{5/2,7/2}$
Fe X	94.012	$3s^23p^5\ ^2P_{3/2} - 3s^23p^4(^1D)4s\ ^2D_{5/2}$
Fe XIV	93.618	$3s^23d\ ^2D_{3/2} - 3s^24p\ ^3P_{1/2}$
Fe XVIII	93.932	$2s^22p^5\ ^2P_{3/2} - 2s2p^6\ ^2S_{1/2}$

Figure 4: The blue and red curves show CHIANTI spectra for an active region (AR; red) and a loop footpoint (TRBR; blue). The dashed line shows the AIA 94 Å channel response curve.

5. SDO/EVE observations

The EUV Variability Experiment (EVE) on board SDO obtains full disk solar spectra over the wavelength region 50-1050 Å at about 1 Å spectral resolution. The solar EUV spectrum is the dominant energy input to the Earth's upper atmosphere, heating the thermosphere and creating the ionosphere, and so it is of crucial importance both to measure the variability and to model the spectrum coming from the Sun.

The solar soft X-ray spectrum (50-170 Å) has never been observed regularly at high spectral resolution, and so efforts at improving the CHIANTI atomic models have focused on comparisons with rocket spectra from the 60s (Del Zanna 2012) and *Chandra* spectra of the star Procyon (Testa et al. 2012), which has a relatively quiet coronal spectrum.

Figure 5 demonstrates the large improvement in the CHIANTI spectra between versions 6 and 7.1, with many new lines that are a good match for the Procyon emission lines.

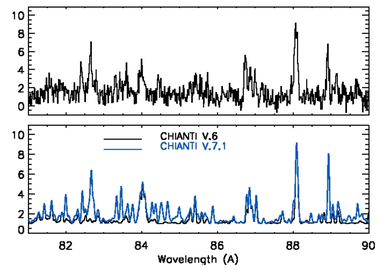

Figure 5: The top panel shows a section of the *Chandra* spectrum of Procyon, and the bottom panel shows synthetic spectra produced with CHIANTI 6 and CHIANTI 7.1.

6. Future Directions

The Hinode/EIS instrument has clearly demonstrated the benefits of high resolution spectra obtained in a wide range of solar conditions, with many new line identifications made, and blends resolved. However, there remains some confusion due to blending amongst lines of Fe VIII to XII, which are always present in solar spectra, while the narrow wavelength sensitivities of EIS miss or poorly observe key spectral regions, particularly 160-180 and 212-245 Å.

New, high resolution laboratory spectra covering a wide wavelength range and with the capability of fine-tuning the plasma energy to focus on individual ion species would be of great benefit in completing line identifications in the EUV and refining the atomic data.

At soft X-ray wavelengths, wide-band, high resolution X-ray spectra are sorely needed from both laboratory and space-borne spectrometers. Del Zanna (2012) noted that no high-resolution solar spectra have been obtained since the 1960s. Atomic data models have progressed beyond the point where they can be reliably tested against these old spectra. If progress is to be made in modeling the solar irradiance spectrum – a crucial input to Earth climate models – then better quality spectra are required.

Data needs:

- High resolution, wide wavelength coverage rocket spectra of soft X-ray (50-170 Å) and short EUV (170-300 Å) regions.
- High resolution, wide wavelength coverage laboratory spectra of soft X-ray and short EUV regions, with capability of adjusting the ionization of the plasma to enhance individual ion species.